Ain Shams Engineering Journal (2014) 5, 85–101

Ain Shams University

Ain Shams Engineering Journal

www.elsevier.com/locate/asej
www.sciencedirect.com

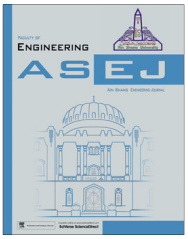

ELECTRICAL ENGINEERING

An opposition-based harmony search algorithm for engineering optimization problems

Abhik Banerjee [a], V. Mukherjee [b,*], S.P. Ghoshal [c]

[a] Department of Electrical Engineering, Asansol Engineering College, Asansol, West Bengal, India
[b] Department of Electrical Engineering, Indian School of Mines, Dhanbad, Jharkhand, India
[c] Department of Electrical Engineering, National Institute of Technology, Durgapur, West Bengal, India

Received 2 March 2013; revised 16 May 2013; accepted 7 June 2013
Available online 19 July 2013

KEYWORDS

Benchmark test function;
Harmony search;
Opposite numbers;
Optimization;
Reactive power compensation

Abstract Harmony search (HS) is a derivative-free real parameter optimization algorithm. It draws inspiration from the musical improvisation process of searching for a perfect state of harmony. The proposed opposition-based HS (OHS) of the present work employs opposition-based learning for harmony memory initialization and also for generation jumping. The concept of opposite number is utilized in OHS to improve the convergence rate of the HS algorithm. The potential of the proposed algorithm is assessed by means of an extensive comparative study of the numerical results on sixteen benchmark test functions. Additionally, the effectiveness of the proposed algorithm is tested for reactive power compensation of an autonomous power system. For real-time reactive power compensation of the studied model, Takagi Sugeno fuzzy logic (TSFL) is employed. Time-domain simulation reveals that the proposed OHS-TSFL yields on-line, off-nominal model parameters, resulting in real-time incremental change in terminal voltage response profile.

1. Introduction

The researchers, over the globe, are being inspired by the nature-inspired meta-heuristics [1] on a regular basis to meet the demands of the real-world optimization problems. The computational costs of the algorithms are being, dramatically, reduced in the recent past.

Being inspired by this tradition, Geem et al. [2] proposed harmony search (HS) in 2001. It is a new variant of derivative-free meta-heuristic algorithm inspired by the natural musical performance process that occurs when a musician searches for a better state of harmony. In the HS algorithm, the solution vector is analogous to the harmony in music and the local and global search schemes are analogous to the musician's improvisations.

In comparison with other meta-heuristics reported in the literature, the HS algorithm imposes fewer mathematical requirements and may be easily adopted for solving various kinds of engineering optimization problems. Furthermore, numerical comparisons demonstrated that the evolution in

* Corresponding author. Tel.: +91 0326 2235644; fax: +91 0326 2296563.
E-mail addresses: abhik_banerjee@rediffmail.com (A. Banerjee), vivek_agamani@yahoo.com (V. Mukherjee), spghoshalnitdgp@gmail.com (S.P. Ghoshal).
Peer review under responsibility of Ain Shams University.

Production and hosting by Elsevier

2090-4479 © 2013 Production and hosting by Elsevier B.V. on behalf of Ain Shams University.
http://dx.doi.org/10.1016/j.asej.2013.06.002

HS algorithm is faster than genetic algorithms [3]. Therefore, the HS algorithm has captured much attention and has been, successfully, applied to solve a wide range of practical optimization problems, such as structural optimization [4], parameter estimation of the nonlinear Muskingum model [5], pipe network design [6], vehicle routing [7], design of water distribution networks [8], and scheduling of a multiple dam system [9].

The HS algorithm is good at identifying the high performance regions of solution space within a reasonable time. A few modified variants of HS were proposed in the literature for enhancing the solution accuracy and the convergence rate. Mahdavi et al. [3] presented an improved HS (IHS) algorithm, by introducing a strategy to dynamically tune the key parameters. Omran and Mahdavi [10] proposed a global best HS (GHS) algorithm, by borrowing the concept from the swarm intelligence. Pan et al. in [11] proposed a self-adaptive global best HS (SGHS) algorithm for solving continuous optimization problems.

Tizhoosh introduced the concept of *opposition-based learning* (OBL) in [12]. This notion has been applied to accelerate the reinforcement learning [13,14] and the back propagation learning [15] in neural networks. The main idea behind OBL is the simultaneous consideration of an estimate and its corresponding opposite estimate (i.e., guess and opposite guess) in order to achieve a better approximation for the current candidate solution. In the recent literature, the concept of opposite numbers has been utilized to speed up the convergence rate of an optimization algorithm, e.g., opposition-based differential evolution (ODE) [16]. This idea of opposite number may be incorporated during the harmony memory (HM) initialization and also for generating the new harmony vectors during the process of HS. In this paper, OBL has been utilized to accelerate the convergence rate of the HS algorithm. Hence, the proposed approach of this paper has been called as opposition-based HS (OHS). OHS uses opposite numbers during HM initialization and also for generating the new HM during the evolutionary process of HS.

The goals of this paper are fourfold.

(a) First, a general presentation of the proposed OHS is given. This has been accomplished by studying the basic HS algorithm including its variants reported in the recent literature.
(b) Second, the proposed OHS algorithm has been tested on a suite of 16 benchmark test functions and the obtained optimal results are compared to other variants of HS reported in the literature like basic HS [2], IHS [3], GHS [10], and SGHS [11]. The comparative convergence profiles of the fitness function values for a few selected benchmark test functions are also presented.
(c) Third, the efficacy of the proposed OHS algorithm has been applied on a real-world power system optimization problem like reactive power compensation of an autonomous hybrid power system model to track its incremental change in terminal voltage real-time under any sort of input perturbation.
(d) And, finally, a statistical analysis is carried out to conclude about the robustness of the comparative algorithms for this power system optimization application.

The rest of the paper is organized as follows. A brief description of HS algorithm is presented in Section 2. A concept of opposition-based learning is presented in Section 3. OHS algorithm is described in Section 4. Pertaining to functional landscape, optimization results of a few benchmark test functions are presented in Section 5. Pertaining to engineering optimization task, reactive power compensation of an autonomous hybrid power system model is focused in Section 6. Finally, Section 7 concludes the present work.

2. A brief description of HS algorithm

2.1. Basic HS algorithm

In the basic HS algorithm, each solution is called a *harmony*. It is represented by an n-dimension real vector. An initial randomly generated population of harmony vectors is stored in an HM. Then, a new candidate harmony is generated from all of the solutions in the HM by adopting a memory consideration rule, a pitch adjustment rule and a random re-initialization. Finally, the HM is updated by comparing the new candidate harmony vector and the worst harmony vector in the HM. The worst harmony vector is replaced by the new candidate vector if it is better than the worst harmony vector in the HM. The above process is repeated until a certain termination criterion is met. Thus, the basic HS algorithm consists of three basic phases. These are initialization, improvisation of a harmony vector, and updating the HM. Sequentially, these phases are described below.

2.1.1. Initialization of the problem and the parameters of the HS algorithm

In general, a global optimization problem can be enumerated as follows: min $f(x)$ s.t. $x_j \in \left[para_j^{\min}, para_j^{\max}\right]$, $j = 1, 2, \ldots, n$ where $f(x)$ is the objective function, $X = [x_1, x_2, \ldots, x_n]$ is the set of design variables; n is the number of design variables. Here, $para_j^{\min}$, and $para_j^{\max}$ are the lower and upper bounds for the design variable x_j, respectively. The parameters of the HS algorithm are the harmony memory size (HMS) (the number of solution vectors in HM), the harmony memory consideration rate ($HMCR$), the pitch adjusting rate (PAR), the distance bandwidth (BW), and the number of improvisations (NI). The NI is the same as the total number of fitness function evaluations (NFFEs). It may be set as a stopping criterion also.

2.1.2. Initialization of the HM

The HM consists of HMS harmony vectors. Let $X_j = [x_1^j, x_2^j, \ldots\ldots, x_n^j]$ represent the jth harmony vector, which is randomly generated within the parameter limits [$para_j^{\min}$, $para_j^{\max}$]. Then, the HM matrix is filled with the HMS harmony vectors as in (1).

$$HM = \begin{bmatrix} x_1^1 & x_2^1 & \ldots\ldots\ x_n^1 \\ x_1^2 & x_2^2 & \ldots\ldots\ x_n^2 \\ \ldots & & \\ x_1^{HMS} & x_2^{HMS} & \ldots\ldots\ x_n^{HMS} \end{bmatrix} \tag{1}$$

2.1.3. Improvisation of a new harmony

A new harmony vector $X^{new} = (x_1^{new}, x_2^{new} \ldots\ldots x_n^{new})$ is generated (called improvisation) by applying three rules viz. (a) a

memory consideration, (b) a pitch adjustment, and (c) a random selection. First of all, a uniform random number r_1 is generated in the range [0, 1]. If r_1 is less than $HMCR$, the decision variable x_j^{new} is generated by the memory consideration; otherwise, x_j^{new} is obtained by a random selection (i.e., random re-initialization between the search bounds). In the memory consideration, x_j^{new} is selected from any harmony vector i in $[1, 2, ldots, HMS]$. Secondly, each decision variable x_j^{new} will undergo a pitch adjustment with a probability of PAR if it is updated by the memory consideration. The pitch adjustment rule is given by (2)

$$x_j^{new} = x_j^{new} \pm r_3 \times BW \tag{2}$$

where r_3 is a uniform random number between 0 and 1.

2.1.4. Updating of HM

After a new harmony vector X_j^{new} is generated, the HM will be updated by the survival of the fitter vector between X^{new} and the worst harmony vector X^{worst} in the HM. That is, X^{new} will replace X^{worst} and become a new member of the HM if the fitness value of X^{new} is better than the fitness value of X^{worst} .

2.1.5. Process of computation

The computational procedure of the basic HS algorithm may be summarized as follows [2]:

HS Algorithm

1. Set the parameters HMS, $HMCR$, PAR, BW, NI, and n.
2. Initialize the HM and calculate the objective function value for each harmony vector.
3. Improvise the HM filled with new harmony X^{new} vectors as follows:

```
for (j = 0; j < n; j++)
  if (r1 < HMCR) then
    x_j^new = x_j^a                          // a ∈ (1, 2, ...., HMS)
      if (r2 < PAR) then
        x_j^new = x_j^new ± r3 × BW          // r1, r2, r3 ∈ [0, 1]
      end if
  else
      x_j^new = para_j^min + r × (para_j^max − para_j^min) // r ∈ [0, 1]
    end if
end for
```

4. Update the HM as $X^{worst} = X^{new}$ if $f(X^{new}) < f(X^{worst})$.
5. If NI is completed, return the best harmony vector X^{best} in the HM; otherwise go back to **Step 3**.

2.2. IHS, GHS, and SGHS algorithms

The basic HS algorithm uses fixed values for PAR and BW parameters. The IHS algorithm, proposed by Mahdavi et al. [3], applies the same memory consideration, pitch adjustment and random selection as the basic HS algorithm but, dynamically, updates the values of PAR and BW as in (3) and (4), respectively.

$$PAR(gn) = PAR^{\min} + \frac{PAR^{\max} - PAR^{\min}}{NI} \times gn \tag{3}$$

$$BW(gn) = BW^{\max} \times e^{\left(\frac{\ln\left(\frac{BW^{\min}}{BW^{\max}}\right)}{NI} \times gn\right)} \tag{4}$$

In (3), $PAR(gn)$ is the pitch adjustment rate in the current generation (gn) and $PAR^{\min}$ and $PAR^{\max}$ are the minimum and the maximum adjustment rate, respectively. In (4), $BW(gn)$ is the distance bandwidth at generation (gn) and $BW^{\min}$ and $BW^{\max}$ are the minimum and the maximum bandwidths, respectively. The details about GHS and SGHS may be found in [10,11].

3. Opposition-based learning: a concept

Evolutionary optimization methods start with some initial solutions (initial population) and try to improve them toward some optimal solution(s). The process of searching terminates when some predefined criteria are satisfied. In the absence of *a priori* information about the solution, we, usually, start with *random guesses*. The computation time, among others, is related to the distance of these initial guesses from the optimal solution. We may improve our chance of starting with a closer (fitter) solution by simultaneously checking *the opposite solution* [12]. By doing this, the fitter one (guess or opposite guess) can be chosen as an initial solution. In fact, according to the theory of probability, 50% of the time a guess is further from the solution than its opposite guess [13]. Therefore, starting with the closer of the two guesses (as judged by its fitness) has the potential to accelerate convergence. The same approach may be applied not only to initial solutions but also continuously to each solution in the current population [13].

3.1. Definition of opposite number

Let $x \in [lb, ub]$ be a real number. The opposite number is defined as in (5).

$$\breve{x} = lb + ub - x \tag{5}$$

Similarly, this definition can be extended to higher dimensions [12] as stated in the next sub-section.

3.2. Definition of opposite point

Let $X = (x_1, x_2, \ldots\ldots, x_n)$ be a point in n-dimensional space, where $(x_1, x_2, \ldots\ldots, x_n) \in R$ and $x_i \in [ub_i, lb_i]\ \forall_i \in \{1, 2, \ldots\ldots, n\}$. The opposite point $\breve{x} = (\breve{x}_1, \breve{x}_2 \ldots\ldots, \breve{x}_n)$ is completely defined by its components as in (6).

$$\breve{x}_i = lb_i + ub_i - x_i \tag{6}$$

Now, by employing the opposite point definition, the opposition-based optimization is defined in the following subsection.

3.3. Opposition-based optimization

Let $X = (x_1, x_2, \ldots\ldots, x_n)$ be a point in n-dimensional space (i.e., a candidate solution). Assume $f = (\cdot)$ is a fitness function which is used to measure the candidate's fitness. According to the definition of the opposite point, $\breve{x} = (\breve{x}_1, \breve{x}_2, \ldots\ldots, \breve{x}_n)$ is the opposite of $X = (x_1, x_2, \ldots\ldots, x_n)$.

Now, if $f(\breve{x}) \leqslant f(X)$, then point X can be replaced with $\breve{x}$; otherwise, we continue with X. Hence, the point and its

opposite point are evaluated simultaneously in order to continue with the fitter one.

4. OHS algorithm

Similar to all population-based optimization algorithms, two main steps are distinguishable for HS algorithm. These are HM initialization and producing new HM by adopting the principle of HS. In the present work, the strategy of OBL [12] is incorporated in two steps. The original HS is chosen as the parent algorithm and opposition-based ideas are embedded in it with an intention to exhibit accelerated convergence profile. Corresponding pseudo code for the proposed OHS approach may be summarized as follows:

OHS Algorithm

1. Set the parameters HMS, $HMCR$, $PAR^{\min}$, $PAR^{\max}$, $BW^{\min}$, $BW^{\max}$, and NI.
2. Initialize the HM with $X_{0_{i,j}}$.
3. **Opposition-based HM initialization**.
  for $(i = 0;\ i < HMS;\ i++)$
    for $(j = 0;\ j < n;\ j++)$
      $OX_{0_{i,j}} = para_j^{\min}$ // OX_0: Opposite of initial X_0
      $+para_j^{\max} - X_{0_{i,j}}$
    end for
  end for
  // **End of opposition-based HM initialization**.

Select HMS fittest individuals from set of $\{X_{0_{i,j}},\ OX_{0_{i,j}}\}$ as initial HM; HM being the matrix of fittest X vectors

4. Improvise a new harmony X^{new} as follows:

Update $PAR(gn)$ by (3) and $BW(gn)$ by (4).

for $(i = 0;\ i < HMS;\ i++)$
  for $(j = 0;\ j < n;\ j++))$
    if $(r_1 < HMCR)$ then
      $X_{i,j}^{new} = X_{i,j}^{a}$ // $a \in (1, 2, \ldots.., HMS)$
      if $(r_2 < PAR(gn))$ then
        $X_{i,j}^{new} = X_{i,j}^{new} \pm r_3$ // $r_1, r_2, r_3 \in [0, 1]$
        $\times BW(gn)$
    end if
  else
    $X_{i,j}^{new} = para_{i,j}^{\min} + r$ // $r \in [0, 1]$
    $\times\left(para_{i,j}^{\max} - para_{i,j}^{\min}\right)$
    end if
  end for
end for

5. Update the HM as $X^{worst} = X^{new}$ if $f(X^{new}) < f(X^{worst})$
6. **Opposition-based generation jumping**
    if $(rand_2 < J_r)$ // $rand_2 \in [0,1]$, J_r: Jumping rate
      for $(i = 0;\ i < HMS;\ i++)$
        for $(j = 0;\ j < n;\ j++)$
          $OX_{i,j} = \min_j^{gn} + \max_j^{gn} - X_{i,j}$

// $\min_j^{gn}$:minimum value of the jth variable in the current generation (gn)
// $\max_j^{gn}$:maximum value of the jth variable in the current generation (gn)

        end for
      end for
  end if

Select HMS fittest HM from the set of $\{X_{i,j}, OX_{i,j}\}$ as current HM.
  // **End of opposition-based generation jumping**.

7. If NI is completed, return the best harmony vector X^{best} in the HM; otherwise go back to **Step 4**.

5. Optimization of benchmark test function (pertaining to functional landscape)

5.1. Benchmark test function

A suite of sixteen global optimization problems are used to test the performance of the proposed OHS algorithm. A detail of each benchmark test function is presented in Appendix Section (Table A.1). Among these sixteen benchmark problems, Sphere function, Schwefel's problem 2.22, Step function, Rotated hyper-ellipsoid function, Shifted Sphere function and Shifted Schwefel's problem 1.2 are unimodal. Step function is discontinuous. Rosenbrock function, Schwefel's problem 2.26, Rastrigin function, Ackley function, Griewank function, Shifted Rosenbrock function, Shifted Rastrigin function, Shifted Rotated Griewank's Function, and Shifted Rotated Rastrigin function are difficult multimodal problems where the number of local optima increases with the problem dimension. Six-hump Camel-back function is a low-dimensional function with only a few local optima.

5.2. Parameter setting

The best chosen variables for the proposed OHS are $J_r = 0.8$, $HMCR = 0.9$, $PAR^{\min} = 0.45$, $PAR^{\max} = 0.98$, $BW^{\min} = 1.00e\text{-}06$, $BW^{\max} = 1/20(para^{\max} - para^{\min})$.

5.3. Discussion on benchmark function optimization

Each benchmark test function is run for 25 independent times. The average and standard deviations over these 25 runs for 30 and 100 dimensions (except for the two-dimensional six-hump Camel-back function) are presented in Tables 1 and 2, respectively. The statistical significant best solutions have been shown in bold face.

It may be observed that the OHS algorithm generates nine best results out of sixteen functions, and for five test functions, OHS and SGHS yield the same results (for dimension size of 30). For two functions like Shifted Rosenbrock function and Shifted rotated Griewank's function, SGHS yields better results than OHS. It may also be noted from Table 2 that with the increase in dimensionality of the benchmark test functions, OHS offers significantly better results than the compared algorithms. Thus, as the dimension, thereby, the complexity of the benchmark test functions increases, OHS offers superior results.

The convergence profiles of the fitness function value ($n = 30$) for (a) Sphere function and (b) Schwefel's problem 2.22 against the NFFEs are presented in Fig. 1a and b, respectively. The HS-, IHS-, GHS-, SGHS-, and OHS-based comparative convergence profiles of the fitness function values ($n = 100$) for 30D Shifted Rastrigin function against NFFEs are presented in Fig. 2. It may be observed from these figures that the convergence profiles of the proposed OHS-based optimum value for these selected test function descend much faster than the other compared algorithms. It points out the fact that the proposed OHS-based results for these benchmark test functions are superior to the other compared methods.

Table 1 Mean and standard deviation (±SD) of the benchmark function optimization results (n = 30).

Function	Global optimum	HS [2]	IHS [3]	GHS [10]	SGHS [11]	OHS
f_1	0	0.000187 ± 0.000032	0.000712 ± 0.000644	0.000010 ± 0.000022	**0**.000000 ± **0**.000000	**0**.000000 ± **0**.000000
f_2	0	0.171524 ± 0.072851	1.097325 ± 0.181253	0.072815 ± 0.114464	0.000102 ± 0.000017	**0**.000101 ± **0**.000013
f_3	0	340.297100 ± 266.691353	624.323216 ± 559.847363	49.669203 ± 59.161192	150.929754 ± 131.054916	**47.36718 ± 130.17368**
f_4	0	4.233333 ± 3.029668	3.333333 ± 2.195956	0 ± 0	**0**.000000 ± **0**.000000	**0**.000000 ± **0**.0000000
f_5	0	4297.816457 ± 1362.148438	4313.653320 ± 1062.106222	5146.176259 ± 6348.792556	11.796490 ± 7.454435	**10**.371876 ± **6**.394781
f_6	0	30.262214 ± 11.960017	34.531375 ± 10.400177	0.041657 ± 0.050361	0.004015 ± 0.006237	**0**.003145 ± **0**.005372
f_7	0	1.390625 ± 0.824244	3.499144 ± 1.182907	0.008629 ± 0.015277	0.017737 ± 0.067494	**0**.001376 ± **0**.001387
f_8	0	1.130004 ± 0.407044	1.893394 ± 0.314610	0.020909 ± 0.021686	0.484445 ± 0.356729	**0.0031678** ± **0**.000136
f_9	0	1.119266 ± 0.041207	1.120992 ± 0.040887	0.102407 ± 0.175640	0.050467 ± 0.035419	**0**.037451 ± **0**.032175
f_{10}	−1.0316285	**−1**.031628 ± **0**.000000	**−1**.031628 ± **0**.000000	−1.031600 ± 0.000018	**−1**.031628 ± **0**.000000	**−1.031628** ± **0**.000000
f_{11}	−450	−443.553193 ± 2.777075	−438.815459 ± 3.703810	1353.211035 ± 361.763223	**−450**.000000 ± **0**.000000	**−450**.000000 ± **0.000000**
f_{12}	−450	3888.178656 ± 1115.259221	3316.602220 ± 1519.408280	18440.504168 ± 4537.943604	−431.095663 ± 17.251617	**−441**.367184 ± **16**.310728
f_{13}	390	3790.700528 ± 3271.573964	5752.122700 ± 3762.543380	35046942.785443 ± 22136432.286008	**2511**.678953 ± **3966**.480932	2817.638432 ± 3841.420371
f_{14}	−330	−329.128972 ± 0.808682	−328.056701 ± 0.667483	−263.271951 ± 9.356208	**−329**.860811 ± **0**.349908	**−329**.860867 ± **0**.349908
f_{15}	−180	547.868607 ± 0.500873	494.756015 ± 6.717343	546.625388547 ± 8686070.613099	**−47**.188943 ± **13**.313494	−58.312701 ± 12.513207
f_{16}	−330	−274.687463 ± 12.863299	−270.694907 ± 16.223212	−192.095804 ± 18.645826	−232.136195 ± 30.033504	**−280**.413671 ± **11**.218671

Table 2 Mean and standard deviation (±SD) of the benchmark function optimization results (n = 100).

Function	Global optimum	HS [2]	IHS [3]	GHS [10]	SGHS [11]	OHS
f_1	0	8.683062 ± 0.775134	8.840449 ± 0.762496	2.230721 ± 0.565271	**0**.000002 ± **0**.000003	**0**.000001 ± **0**.000002
f_2	0	82.926284 ± 6.717904	82.548978 ± 6.341707	19.020813 ± 5.093733	0.017581 ± 0.021205	**0**.015438 ± **0**.020179
f_3	0	16675172.184717 ± 3182464.488466	17277654.059718 ± 2945544.275052	2598652.617273 ± 915937.797217	621.749360 ± 583.889593	**619**.753628 ± **581.334539**
f_4	0	20280.200000 ± 2003.829956	20827.733333 ± 2175.284501	5219.933333 ± 1134.876027	0.100000 ± 0.305129	**0.091036** ± **0.300141**
f_5	0	215052.904398 ± 28276.375538	213812.584732 ± 28305.249583	321780.353575 ± 39589.041160	37282.096600 ± 5913.489066	**37173.001346** ± **5910.331444**
f_6	0	7960.925495 ± 572.390489	8301.390783 ± 731.191869	1270.944476 ± 395.457330	35.675398 ± 86.000104	**33.413687** ± **85.100030**
f_7	0	343.497796 ± 27.245380	343.232044 ± 25.149464	80.657677 ± 30.368471	12.353767 ± 2.63560	**11.100003** ± **2.543010**
f_8	0	13.857189 ± 0.284945	13.801383 ± 0.530388	8.767846 ± 0.880066	**−0.000000** ± **0.000000**	**−0.000000** ± **0.000000**
f_9	0	195.592577 ± 24.808359	204.291518 ± 19.157177	54.252289 ± 18.600195	0.027932 ± 0.009209	**0.021349** ± **0.008312**
f_{11}	−450	22241.554607 ± 2550.746480	23026.241628 ± 2304.787587	88835.245672 ± 9065.418923	−449.999980 ± 0.000093	**−450.000000** ± **0.000072**
f_{12}	−450	272495.060293 ± 38504.505752	274439.336302 ± 37300.950900	496668.916387 ± 51929.415486	63251.604588 ± 12430.053431	**63248.112343** ± **12428.04301**
f_{13}	390	2242245818.867268 ± 380621042.775803	2211121263.779596 ± 358676387.353021	27910012932.716747 ± 3941689420.106002	781.510290 ± 293.228166	**776.423648** ± **285.210031**
f_{14}	−330	36.164513 ± 25.576559	36.685585 ± 25.311496	509.066964 ± 45.183819	−317.225748 ± 2.732871	**−319.201033** ± **2.436781**
f_{15}	−180	1885.100054 ± 12.499888	1883.499365 ± 15.485959	1829.669549 ± 33.504803	1006.117891 ± 35.307793	**1004.231340** ± **34.172839**
f_{16}	−330	341.676241 ± 48.372925	334.747556 ± 54.693700	763.818874 ± 43.613654	66.915779 ± 55.375297	**46.310278** ± **53.112855**

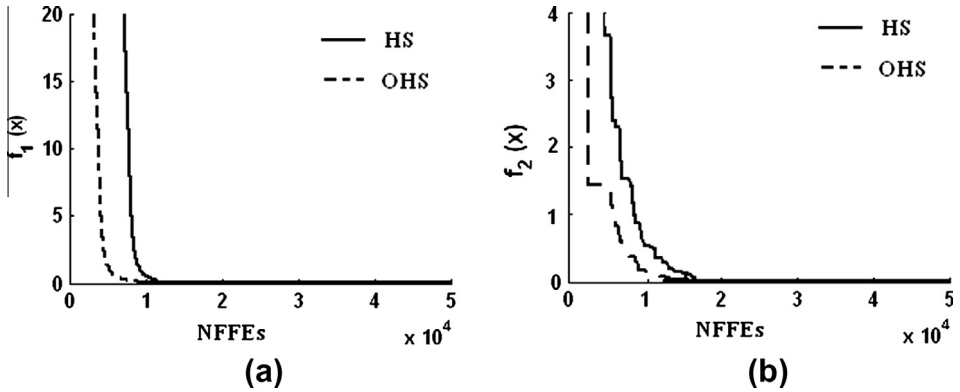

Figure 1 Comparative convergence profiles of the fitness function values for the 30D. (a) Sphere function. (b) Schwefel's problem 2.22.

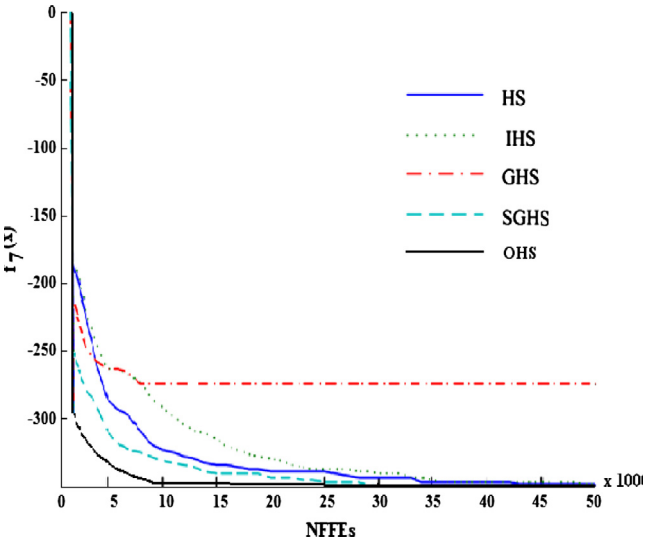

Figure 2 Comparative convergence profiles of the fitness function values for the shifted 30D Rastrigin function.

6. Reactive power compensation of an autonomous hybrid power system model (pertaining to engineering optimization application)

6.1. General

The main advantages of using renewable energy sources are that these are clean in nature, sustainable, and eco-friendly. In modern power system, there has been a continuous enhancement of power generation from renewable energy sources like solar energy, wind energy etc. Wind energy is intermittent and fluctuating in nature. Thus, power generation from wind is variable. To reduce the fluctuation of wind generation, wind power generations are, generally, designed to operate in parallel with diesel generators [17]. This combination of diesel and wind energy system is known as wind–diesel hybrid power system.

Thus, in general, there may be more than one type of electrical generators in any hybrid energy system [18]. In such circumstances, it is normal although not essential for diesel engine-based generator(s), usually, to be synchronous generator (SG) and wind-turbine-based generator(s) to be asynchronous such as induction generator (IG). An IG offers many advantages over the conventional SG as a source of isolated power supply. Reduction in unit cost, ruggedness, absence of brushes (in squirrel cage construction), absence of separate DC source for excitation, easy maintenance, self protection against severe overloads and short circuits, etc. are the main advantages of an IG [19] but it requires reactive power support for its operation. Due to this mismatch between generation and consumption of reactive powers, more voltage fluctuations occur at generator terminal in an isolated system which reduces the stability and quality of supply. The problem becomes more complicated in hybrid system having both IGs and SGs. In the present investigated hybrid power system model, SG and IG are chosen with diesel generator and wind turbine, respectively.

Various flexible AC transmission system (FACTS) devices are available which may supply fast and continuous reactive power support [20]. For standalone applications, effective capacitive VAR controller has become central to the success of IG system. Switched capacitors, static VAR compensator (SVC), and static synchronous compensator may provide the requisite amount of reactive power support.

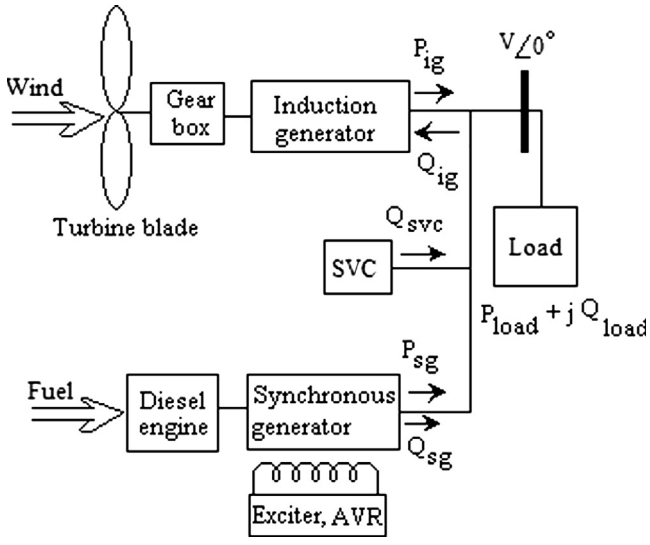

Figure 3 Single-line diagram of the studied isolated wind–diesel power system.

6.2. Studied hybrid power system model

The studied hybrid wind–diesel power system comprises of the SG coupled with a diesel engine, IG coupled with a wind turbine, electrical loads and reactive power compensating device such as SVC [20,21] and a control mechanism. Fig. 3 depicts the single line diagram of the studied hybrid power system model. It is to be noted here that both the SG and the IG fulfill the active power demanded by the load, while the reactive power requirement for the operation of the IG and that of the load is provided by the SG and the SVC. The real and reactive power demand equations for the studied power system model, in *s*-domain, may be modeled as in the following equation:

$$\Delta P_{ig}(s) + \Delta P_{sg}(s) - \Delta P_{load}(s) = 0 \tag{7}$$

$$\Delta Q_{sg}(s) + \Delta Q_{sc}(s) - \Delta Q_{load}(s) - \Delta Q_{ig}(s) = 0 \tag{8}$$

Any sort of disturbance in the reactive power demanded by the load (ΔQ_{load}) may lead to the system voltage change which, in turn, results in incremental change in reactive power demand of the other components. The left hand side of (8) represents the net incremental reactive power surplus and this surplus in reactive power demand will have its immediate effect

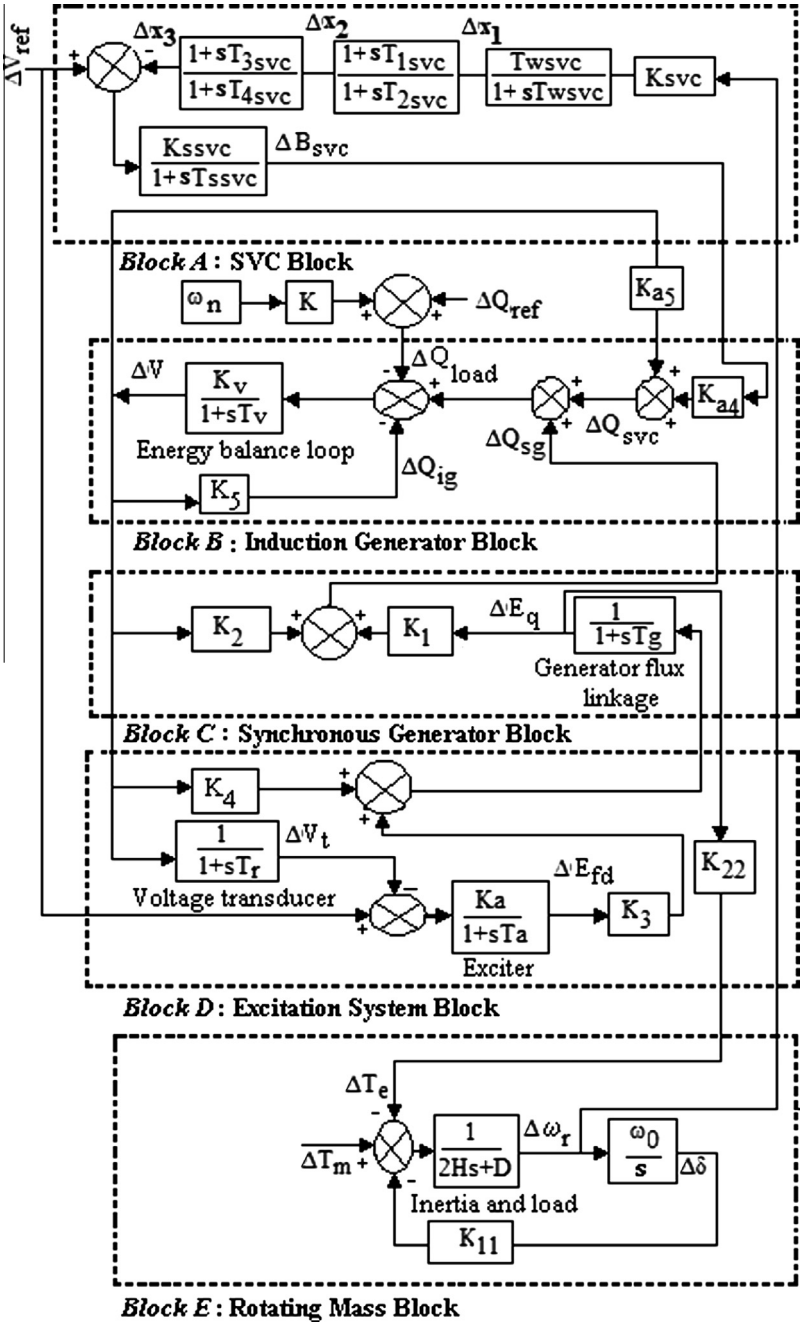

Figure 4 Transfer-function block diagram for reactive power control of the studied wind–diesel hybrid power system.

on the change in system voltage. But as per the recommendation of the grid, the voltage change should be within its permissible limit. This necessitates that the terminal voltage profile should be maintained properly.

Fig. 4 depicts the transfer-function block diagram for the reactive power control of the studied wind–diesel hybrid power system model. From this figure, the governing transfer function equation for the incremental change in load voltage (ΔV) may be written, in s-domain, as in the following equation:

$$\Delta V(s) = \left(\frac{K}{1+sT}\right)[\Delta Q_{sg}(s) + \Delta Q_{sc}(s) - \Delta Q_{load}(s) - \Delta Q_{ig}(s)] \quad (9)$$

6.2.1. Modeling of the SG (Block C, Fig. 4)

The incremental change in reactive power of the SG may be given by the following equation:

$$\Delta Q_{sg}(s) = K_1 \Delta E_q(s) + K_2 \Delta V(s) \quad (10)$$

where

$$K_1 = \frac{V\cos\delta}{X'_d} \quad (11)$$

$$K_2 = \frac{(E'\cos\delta - 2V)}{X'_d} \quad (12)$$

It is to be noted here that $\Delta E_q(s)$ is proportional to the change in the direct axis field flux under steady state condition and is given below for the small perturbation by solving the equation of flux linkages as stated in (13)

$$\Delta E_q(s) = \left(\frac{1}{1+sT_g}\right)[K_3 \Delta E_{sg}(s) + K_4 \Delta V(s)] \quad (13)$$

$$\text{where} \quad K_3 = \frac{X'_d}{X_d} \quad (14)$$

$$K_4 = \frac{\left[\left(X_d - X'_d\right)\cos\delta\right]}{X'_d} \quad (15)$$

$$\text{and} \quad T_g = T'_{d0}\frac{X'_d}{X_d} \quad (16)$$

6.2.2. Modeling of the IG (Block B, Fig. 4)

The reactive power requirement of an IG under constant slip condition (S) in terms of generator terminal voltage and generator parameters is given by the following equation:

$$\Delta Q_{ig}(s) = K_5 \Delta V(s) \quad (17)$$

where

$$K_5 = \frac{2VX_{eq}}{\left(R_Y^2 + X_{eq}^2\right)} \quad (18)$$

$$R_Y = R_p + R_{eq} \quad (19)$$

$$R_p = \frac{r'_2}{S}(1-S) \quad (20)$$

$$R_{eq} = r_1 + r'_2 \quad (21)$$

$$X_{eq} = x_1 + x'_2 \quad (22)$$

where r_1, x_1, r'_2 and x'_2 are the parameters of the IG.

6.2.3. Modeling of SVC (Block A, Fig. 4)

In wind–diesel hybrid power system, IG draws reactive power. Apart from that, the most of the loads are inductive in nature and the inductive loads also draw reactive power from the line. So, there is always a chance of deficit of reactive power in the studied model. In the present work, SVC is used to control the generator terminal voltage of the wind–diesel hybrid power system model by compensating the mismatch between reactive power generation and demand [20,21]. The block diagram of SVC, as adopted in the present work, is shown in *Block A* of Fig. 4.

6.3. Mathematical problem formulation

6.3.1. Measure of performance

Two performance indices like integral absolute error (*IAE*), and integral square error (*ISE*) are considered in the present work and the definitions of these two are as follows in (23) and (24), respectively.

$$IAE = \int_0^\infty |V_t(t)|dt \quad (23)$$

$$ISE = \int_0^\infty V_t^2(t)dt \quad (24)$$

6.3.2. Design of figure of demerit

The objective of the present work is to achieve the minimal incremental change in terminal voltage (ΔV_t (p.u.)) response profile following any sort of power system disturbances. This may be achieved when minimized overshoot (M_p), minimized settling time (t_s), lesser rising time (t_r), and lesser steady state error (E_{ss}) of the transient response profile are achieved. Thus, a time-domain performance index, called as figure of demerit (*FOD*), is designed as in (25) [22].

$$FOD = (1 - e^{-\gamma})(M_p + E_{ss}) + e^{-\gamma}(t_s - t_r) \quad (25)$$

In the present work, the value of γ is set as 1.0 [22].

6.3.3. Constraints of the problem

The constrained optimization problem for the tuning of the parameters of the studied isolated hybrid power system model is subject to the limits of the different tunable parameters as presented in Table 3.

Table 3 Range of SVC parameters.

SVC parameters	Minimum value	Maximum value
K_{svc}	10.0	100.0
K_{ssvc}	10.0	100.0
T_{wsvc}	0.005	0.05
T_{1svc}	0.005	0.05
T_{2svc}	0.005	0.05
T_{3svc}	0.005	0.05
T_{4svc}	0.005	0.05
T_{ssvc}	0.005	0.05

6.3.4. Formulation of mathematical optimization problem

The optimization task of the present work is taken as minimization of a performance index, integral square time error (ISTE) [22] as stated as in the following equation:

$$Min\ P_{index} = Min\ [ISTE] = Min\left[\int_0^{\infty} t \times V_t^2(t)dt\right] \tag{26}$$

The optimal values of the tunable parameters of the studied isolated hybrid power system model are obtained by minimizing the value of P_{index} given in (26) with the help of any of the optimizing techniques with due regard to the constraints of the model. And, subsequently, the values of *IAE*, *ISE*, and *FOD* are obtained with the help of (23)–(25), in sequence, by utilizing the optimal controller parameters as yielded by any of the adopted optimization algorithm.

6.4. Review of Takagi Sugeno fuzzy logic (TSFL) for on-line tuning of controller gains

The whole process of TSFL [23] involves three steps as:

(a) *Fuzzification*: The first step is fuzzification of input operating conditions as load voltage (V) and equivalent reactance (X_{eq}), in terms of fuzzy subsets (Low (L), Medium (M), High (H)). These are associated with overlapping triangular membership functions. TSFL rule base table is formed, each composed of two nominal inputs and corresponding nominal optimal SVC parameters as output determined by any of the optimizing techniques dealt with. The respective nominal central values of the input subsets of V are (0.5, 0.8, 1.1), while those for X_{eq} are (0.4752, 0.77, 1.08), respectively, at which membership values are unity (Fig. 5). These are nominal input conditions also. Sugeno fuzzy rule base table consists of $3^2(=9)$ logical input conditions or sets (TSFL tables calculated for the SVC structures investigated), each composed of two nominal inputs. Each logical input set corresponds to nominal optimal SVC parameters as output.

(b) *Sugeno fuzzy inference*: For on-line imprecise values of input parameters, firstly their subsets in which the values lie are determined with the help of "IF", "THEN" logic and corresponding membership values are determined from the membership functions of the subsets. From Sugeno fuzzy rule base table, corresponding input sets and nominal SVC parameters are determined. Now, for each input set being satisfied, two membership values like μ_V and $\mu_{X_{eq}}$ and their minimum $\mu_{\min}$ are computed. For the input logical sets, which are not satisfied because parameters do not lie in the corresponding fuzzy subsets, $\mu_{\min}$ will be zero. For the non-zero $\mu_{\min}$ values only, nominal SVC parameters corresponding to fuzzy sets being satisfied are taken from the Sugeno fuzzy rule base table.

(c) *Sugeno defuzzification*: It yields the defuzzified, crisp output for each parameter of SVC. Final crisp SVC parameter output is given by the following equation:

$$K_{crisp} = \frac{\sum_i \mu_{\min}^{(i)} \cdot K_i}{\sum_i \mu_{\min}^{(i)}} \tag{27}$$

where i corresponds to input logical sets being satisfied among 9 input logical sets and K_i is corresponding nominal SVC parameter. K_{crisp} is crisp SVC parameter. $\mu_{\min}^{(i)}$ is the minimum membership value corresponding to ith input logical set being satisfied.

6.5. Simulation results and discussions

The values for the different constants of the studied hybrid power system model are presented in Appendix Section.

6.5.1. Test cases considered

The state differential equations in standard from may be written as in the following equation:

$$\Delta\dot{X} = A\Delta\underline{X} + B\Delta\underline{U} + \Gamma\Delta\underline{P} \tag{28}$$

where ΔX, ΔU and ΔP are the state, control and disturbance vectors, respectively, while A, B and Γ are the system, control and disturbance matrices, respectively. Based on Fig. 4, the following two test cases are considered in the present work.

- *Case I*: Only model (i.e., SVC block is absent in Fig. 4).

The different vector components of the standard state differential equations for this test case as expressed in (27) are given by the following equation:

$$\Delta\underline{X} = [\Delta\omega_r \quad \Delta\delta \quad \Delta E_{fd} \quad \Delta E_q \quad \Delta V_t \quad \Delta V]^T \tag{29}$$

$$\Delta\underline{U} = [\Delta V_{ref} \quad \Delta T_m]^T \tag{30}$$

$$\Delta\underline{P} = [\Delta Q_{ref}] \tag{31}$$

There are no as such tunable parameters for this test case.

- *Case II*: Model + SVC (i.e., the SVC block is present in Fig. 4).

The different vector components of the standard state differential equations for this test case as expressed in (27) are given by the following equation:

$$\Delta\underline{X} = [\Delta\omega_r \quad \Delta\delta \quad \Delta E_{fd} \quad \Delta E_q \quad \Delta V_t \quad \Delta V \quad \Delta x_1 \quad \Delta x_2 \quad \Delta x_3 \quad \Delta B_{sc}]^T \tag{32}$$

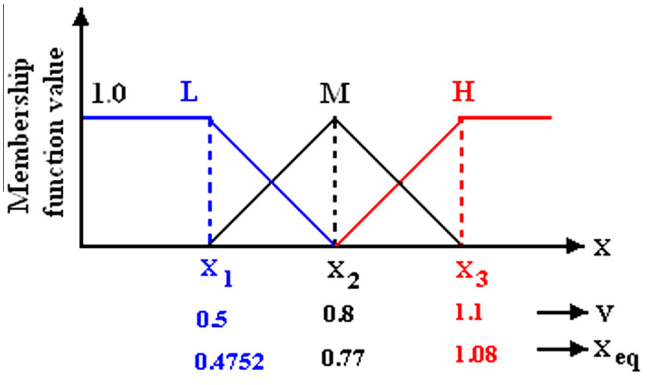

Figure 5 Fuzzification of input operating conditions (V and X_{eq}).

Table 4 Sample Takagi–Sugeno fuzzy rule base table for Case II (Model + SVC).

Input operating condition V, X_{eq} (both are in p.u.)	Algorithm	Optimal model parameters (K_{svc}, K_{ssvc}, T_{wsvc}, T_{1svc}, T_{2svc}, T_{3svc}, T_{4svc}, T_{ssvc})	*IAE*	*ISE*	P_{index}
1.01, 0.93	BGA	27.92, 10.70, 0.0101, 0.0430, 0.0438, 0.0087, 0.0447, 0.0080	221.2256	5.2601	0.7948
	IHS	17.63, 11.35, 0.0250, 0.0061, 0.0291, 0.0093, 0.0388, 0.0054	220.7069	5.0631	0.7878
	HS	15.31, 10.11, 0.0210, 0.0051, 0.0271, 0.0064, 0.0410, 0.0048	220.1001	5.0510	0.7800
	OHS	13.45, 11.03, 0.0280, 0.0050, 0.0497, 0.0050, 0.0493, 0.0052	**219.5233**	**5.0164**	**0.7783**
1.01, 1.08	BGA	25.82, 11.05, 0.0055, 0.0059, 0.0474, 0.0071, 0.0154, 0.0050	216.7345	5.4978	0.7795
	HS	16.20, 11.13, 0.0316, 0.0078, 0.0500, 0.0050, 0.0389, 0.0089	215.1551	5.3210	0.7731
	IHS	19.15, 10.47, 0.0245, 0.0054, 0.0416, 0.0041, 0.02156, 0.0049	213.1400	5.3012	0.7612
	OHS	26.06, 10.64, 0.0500, 0.0050, 0.0500, 0.0050, 0.0500, 0.0050	**212.6082**	**5.2612**	**0.7566**
1.01, 0.4752	BGA	10.70, 10.00, 0.0062, 0.0196, 0.0363, 0.0052, 0.0479, 0.0094	253.5136	4.9910	0.8801
	HS	15.67, 11.72, 0.0429, 0.0138, 0.0402, 0.0050, 0.0086, 0.0146	254.2652	4.8946	0.8624
	IHS	14.17, 10.49, 0.0521, 0.0061, 0.0514, 0.0049, 0.0074, 0.0064	251.4569	4.8712	0.8512
	OHS	30.63, 10.00, 0.0474, 0.0052, 0.0500, 0.0063, 0.0480, 0.0054	**248.7237**	**4.8078**	**0.8308**
1.0, 0.93	BGA	19.49, 11.75, 0.0252, 0.0057, 0.0484, 0.0119, 0.0495, 0.0099	227.6804	5.2115	0.7896
	HS	20.37, 12.04, 0.0070, 0.0489, 0.0285, 0.0169, 0.0397, 0.0055	217.0124	5.0171	0.7763
	IHS	24.10, 10.89, 0.0045, 0.0047, 0.0512, 0.0078, 0.0415, 0.0061	216.1409	5.0101	0.7612
	OHS	23.16, 10.00, 0.0500, 0.0050, 0.0496, 0.0050, 0.0494, 0.0050	**215.4302**	**5.0010**	**0.7516**
1.0, 1.08	BGA	18.43, 11.40, 0.0057, 0.0208, 0.0488, 0.0099, 0.0294, 0.0117	214.0409	5.4708	0.7813
	HS	20.52, 11.41, 0.0050, 0.0220, 0.0210, 0.0261, 0.0432, 0.0053	211.7528	5.2054	0.7735
	IHS	21.14, 10.91, 0.0046, 0.0198, 0.0239, 0.0289, 0.0501, 0.0067	211.0001	5.1749	0.7612
	OHS	23.06, 10.00, 0.0433, 0.0051, 0.0500, 0.0050, 0.0483, 0.0052	**210.6177**	**5.1156**	**0.7472**
1.0, 0.4752	BGA	24.41, 11.40, 0.0150, 0.0080, 0.0391, 0.0073, 0.0484, 0.0057	248.0023	4.9470	0.8474
	HS	13.91, 11.43, 0.0362, 0.0140, 0.0352, 0.0118, 0.0500, 0.0050	247.4704	4.8274	0.8441
	IHS	19.45, 12.46, 0.0456, 0.0096, 0.0465, 0.0236, 0.0519, 0.0041	246.1987	4.8012	0.8312
	OHS	25.66, 10.00, 0.0500, 0.0076, 0.0500, 0.0056, 0.0500, 0.0050	**245.7970**	**4.7143**	**0.8158**
0.99, 0.93	BGA	42.34, 12.81, 0.0131, 0.0148, 0.0489, 0.0106, 0.0440, 0.0071	209.3613	5.3039	0.7645
	HS	43.04, 12.09, 0.0051, 0.0050, 0.0319, 0.0298, 0.0453, 0.0050	207.3805	5.1216	0.7512
	IHS	13.19, 13.18, 0.0415, 0.0049, 0.0418, 0.0196, 0.0346, 0.0089	206.0007	5.1002	0.7319
	OHS	17.51, 10.07, 0.0442, 0.0083, 0.0500, 0.0051, 0.0500, 0.0050	**206.9720**	**5.0342**	**0.7252**
0.99, 1.08	BGA	17.38, 10.00, 0.0205, 0.0171, 0.0496, 0.0148, 0.0280, 0.0057	204.0092	5.6309	0.7381
	HS	18.57, 10.05, 0.0436, 0.0169, 0.0500, 0.0050, 0.0376, 0.0064	202.6559	5.4365	0.7286
	IHS	17.46, 11.19, 0.0085, 0.0094, 0.0614, 0.0078, 0.0417, 0.0049	201.1800	5.4102	0.7277
	OHS	13.98, 13.38, 0.0467, 0.0050, 0.0499, 0.0051, 0.0414, 0.0051	**200.2607**	**5.0175**	**0.7244**
0.99, 0.4752	BGA	24.06, 13.16, 0.0110, 0.0052, 0.0444, 0.0365, 0.0386, 0.0117	240.2984	4.9295	0.8336
	HS	11.72, 10.05, 0.0050, 0.0316, 0.0481, 0.0073, 0.0440, 0.0056	238.9619	4.8996	0.8025
	IHS	18.20, 12.14, 0.0146, 0.0469, 0.0358, 0.0039, 0.0555, 0.0114	237.1984	4.8146	0.7948
	OHS	19.85, 10.04, 0.0500 0.0070, 0.0499, 0.0051, 0.0499, 0.0050	**236.4079**	**4.7859**	**0.7761**

$$\Delta \underline{U} = [\Delta V_{ref} \quad \Delta T_m]^T \tag{33}$$

$$\Delta \underline{P} = [\Delta Q_{ref}] \tag{34}$$

The tunable parameters for this test case are K_{svc}, K_{ssvc}, T_{wsvc}, T_{1svc}, T_{2svc}, T_{3svc}, T_{4svc}, and T_{ssvc}.

6.5.2. Parameter setting

(a) *For BGA*: Number of parameters depends on the model under study (viz. *Case I* and *Case II*)[1], number of bits = (number of parameters) × 8 (for binary coded BGA, as considered in the present work), population size = 60, number of the fitness function evaluations (NFFEs) = 500, mutation probability = 0.001, cross-over rate = 80%.

(b) *For HS, IHS and OHS*: The best chosen variables for the proposed OHS are $HMS = 60$; $HMCR = 0.9$; $PAR^{\min} = 0.45$; $PAR^{\max} = 0.98$; $BW^{\min} = 0.00005$; $BW^{\max} = 50$; $NI = 500$ and n (number of parameters to be optimized); jumping rate, $J_r = 0.8$; NFFEs = 500.

(c) *For the studied power system model*: The values for the different constants of the studied hybrid power system model are presented in Appendix Section.

6.5.3. Discussion on results

The simulation is carried out based on varying load voltage (V, in p.u.) and equivalent reactance (X_{eq}, in p.u.). For time-domain plots of the ΔV_t (in p.u.) in MATLAB-SIMULINK, input step perturbation of 0.01 p.u. is applied either in incremental change in reference voltage (ΔV_{ref}) or in incremental change in mechanical torque (ΔT_m). All the simulations of the present work are carried out based on the same number

[1] There is no as such tunable parameter in *Case I*.

NFFEs. The results of interest **bold faced** in the respective tables. The major observations of the present work are presented below.

(a) *Performance analysis based on* P_{index}: Table 4 includes nine different sets of nominal input conditions on sample basis (for test Case II) of the investigated power system model. This table presents the optimal parameter values for these nine sets of nominal input conditions (for test Case II). It may be noted here that for test Case I, there is no as such tunable parameters. The value of P_{index} for test Case I is recorded as 1.0852. All the contents of this table for test Case II form the Takagi–Sugeno rule base table on sample basis. From Table 4, it may be observed that the value of P_{index} is less for test Case II as compared to test Case I. It is due to the reactive power compensation yielded by the SVC block and, thus, minimized incremental change in terminal voltage is noted. From this table, it may also be noted that the proposed OHS-based optimization technique offers lesser value of P_{index} as compared to either HS-, or IHS-, or BGA-based technique for test Case II. It is observed that the value of P_{index} is the least one for the proposed OHS-based approach, establishing the optimization performance of OHS-based approach to be the best one among the others for this power system application.

(b) *Performance analysis based on FOD:* The performance of the incremental changes in terminal voltages (in terms of M_p, E_{ss}, t_s, t_r, etc.) of the studied hybrid power system model for the adopted approaches are also calculated and presented in Table 5. The value of *FOD* for test case I is recorded as 0.9942. The value of *FOD* is less for test Case II (for any of the adopted approaches) as compared to test Case I which indicates improvement in voltage profile has occurred. From this table, it may also be noted that the value of the *FOD* is the minimum for the OHS-based approach which indicates that the best optimal voltage response profile is achieved for this

Table 5 Comparative performance analysis of the comparative algorithms for Case II (Model + SVC).

Input operating condition V, X_{eq} (both are in p.u.)	Algorithm	Rise time t_r (s)	Over shoot M_p (%)	Steady state error E_{ss}	*FOD*
1.01, 0.93	BGA	0.0960	0.0301	0.0085	0.3569
	HS	0.0963	0.0295	0.0088	0.3567
	IHS	0.0963	0.0294	0.0086	0.3566
	OHS	0.0963	0.0294	0.0083	**0.3563**
1.01, 1.08	BGA	0.0937	0.0315	0.0082	0.3592
	HS	0.0937	0.0321	0.0086	0.3586
	IHS	0.0936	0.0320	0.0087	0.3585
	OHS	0.0935	0.0319	0.0092	**0.3581**
1.01, 0.4752	BGA	0.1095	0.0204	0.0077	0.3479
	HS	0.1091	0.0213	0.0092	0.3470
	IHS	0.1090	0.0210	0.0090	0.3461
	OHS	0.1108	0.0206	0.0086	**0.3456**
1.0, 0.93	BGA	0.0951	0.0305	0.0087	0.3597
	HS	0.0955	0.0300	0.0083	0.3589
	IHS	0.0955	0.0299	0.0082	0.3584
	OHS	0.0954	0.0300	0.0081	**0.3575**
1.0, 1.08	BGA	0.0924	0.0332	0.0081	0.3600
	HS	0.0935	0.0322	0.0081	0.3590
	IHS	0.0934	0.0321	0.0080	0.3586
	OHS	0.0933	0.0320	0.0080	**0.3581**
1.0, 0.4752	BGA	0.1096	0.0205	0.0205	0.3498
	HS	0.1101	0.0205	0.0085	0.3487
	IHS	0.1100	0.0204	0.0085	0.3480
	OHS	0.1100	0.0203	0.0083	**0.3458**
0.97, 0.93	BGA	0.0943	0.0321	0.0093	0.3593
	HS	0.0943	0.0318	0.0084	0.3586
	IHS	0.0942	0.0317	0.0083	0.3579
	OHS	0.0941	0.0316	0.0082	**0.3561**
0.97, 1.08	BGA	0.0920	0.0352	0.0084	0.3686
	HS	0.0920	0.0353	0.0090	0.3670
	IHS	0.0920	0.0350	0.0089	0.3650
	OHS	0.0919	0.0336	0.0087	**0.3610**
0.97, 0.4752	BGA	0.1072	0.0220	0.0085	0.3478
	HS	0.1077	0.0215	0.0076	0.3467
	IHS	0.1076	0.0214	0.0075	0.3461
	OHS	0.1074	0.0213	0.0071	**0.3449**

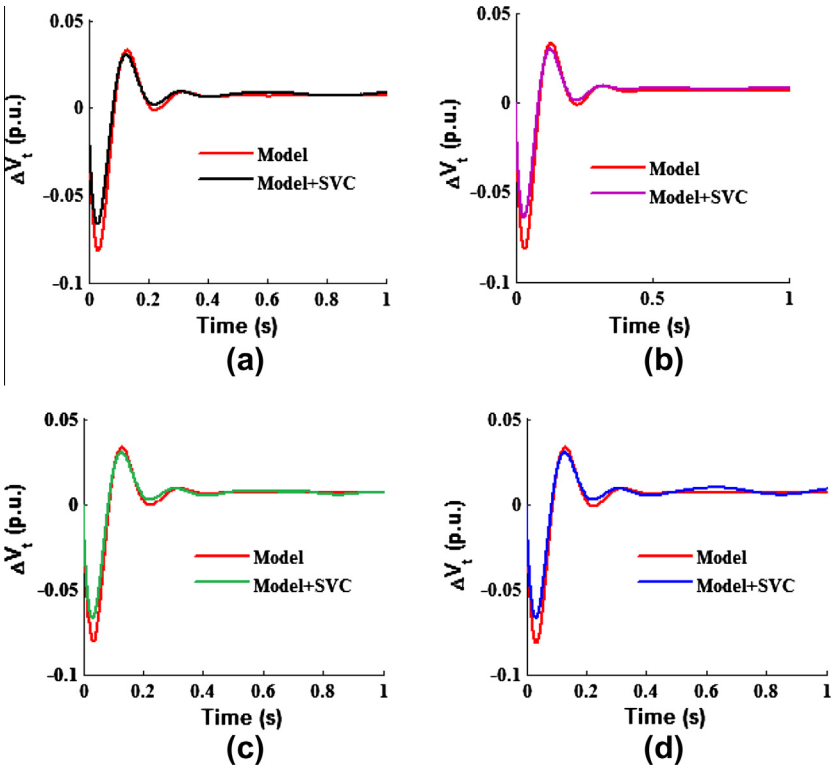

Figure 6 Comparative time-domain simulation responses of the incremental change in terminal voltage (p.u.) for nominal input conditions (V = 1.0 p.u., X_{eq} = 0.93 p.u.) based on the algorithms like (a) BGA, (b) HS, (c) IHS and (d) OHS.

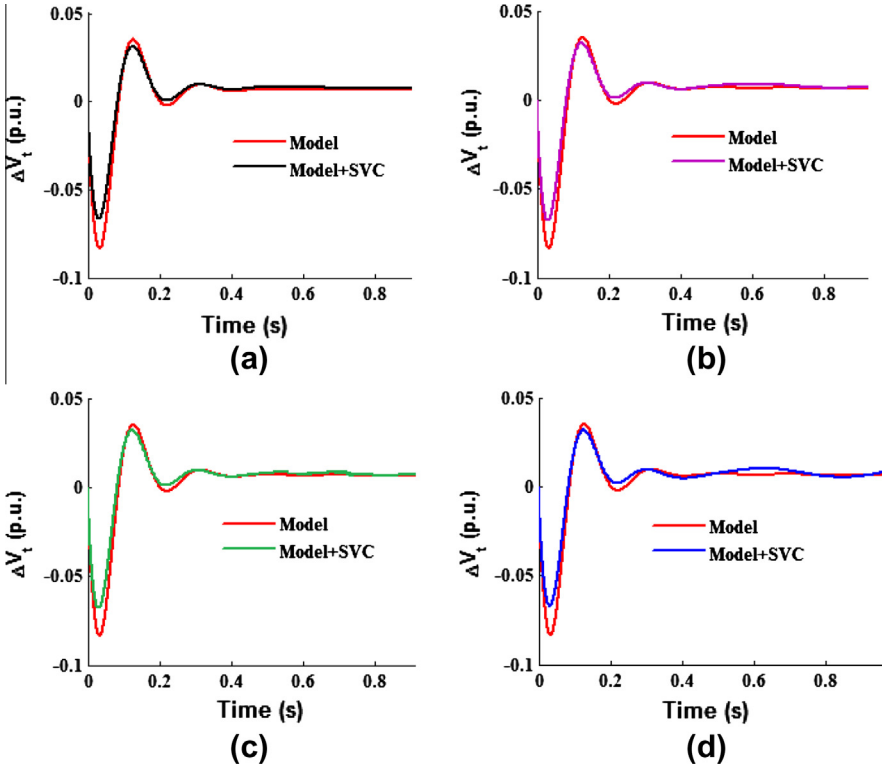

Figure 7 Comparative time-domain simulation responses of the incremental change in terminal voltage (p.u.) for nominal input conditions (V = 1.01 p.u., X_{eq} = 1.08 p.u.) based on the algorithms like (a) BGA, (b) HS, (c) IHS, and (d) OHS.

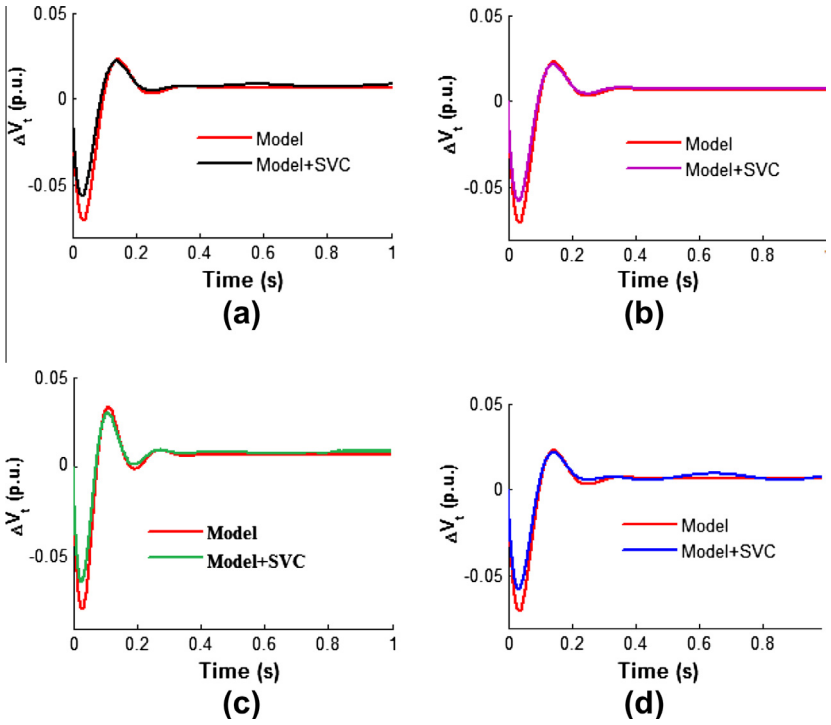

Figure 8 Comparative time-domain simulation responses of the incremental change in terminal voltage (p.u.) for off-nominal input conditions (V = 0.992 p.u., X_{eq} = 1.08 p.u.) based on the algorithms like (a) BGA-TSFL , (b) HS-TSFL , (c) IHS-TSFL, and (d) OHS-TSFL.

Table 6 Takagi–Sugeno fuzzy-based off-nominal, on-line optimal controller gains and transient response characteristics of incremental change in terminal voltage (using BGA/HS/OHS-based optimal gains of Table 4) for Case II viz. (Model + SVC).

Input operating condition V, X_{eq} (both are p.u.)	Algorithm	Optimal model parameters (K_{svc}, K_{ssvc}, T_{wsvc}, T_{1svc}, T_{2svc}, T_{3svc}, T_{4svc}, T_{ssvc})	*FOD*	*IAE*	*ISE*	P_{index}
0.992, 1.08	BGA-TSFL	12.10, 11.40, 0.0210, 0.0268, 0.0208, 0.0050, 0.0257, 0.0168	0.3620	213.8230	5.7912	0.7898
	HS-TSFL	12.49, 10.97, 0.0269, 0.0079, 0.0453, 0.0071, 0.0305, 0.0050	0.3599	210.3729	5.6067	0.7526
	IHS-TSFL	11.91, 10.01, 0.0291, 0.0071, 0.0431, 0.0069, 0.0051, 0.0051	0.3589	209.1458	5.5004	0.7511
	OHS-TSFL	11.03, 10.00, 0.0500, 0.0050, 0.0498, 0.0054, 0.0495, 0.0054	**0.3570**	**208.3964**	**5.4721**	**0.7410**

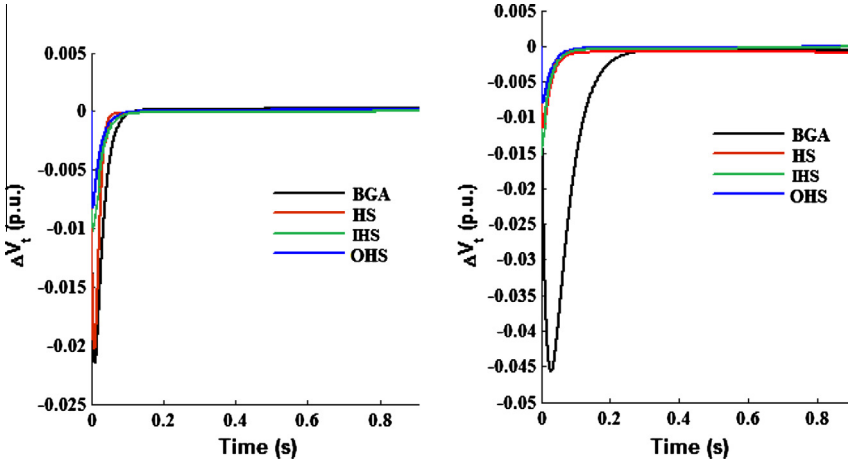

Figure 9 Comparative BGA-, HS-, IHS-, and OHS-based time-domain simulation responses of the incremental change in terminal voltage (p.u.) for test Case II and nominal input conditions like (a) V = 1.01 p.u., X_{eq} = 0.4752 p.u. and (b) V = 1.0 p.u., X_{eq} = 0.93 p.u.

approach. Thus, the OHS-based optimization technique yields optimal voltage response profile and, thus, its optimization performance is found to be better than either IHS-, or HS-, or BGA-based counterparts.

(c) *Performance analysis based on performance indices*: As a measure of performances of the comparative algorithms and the adopted test cases, the values of *IAE* and *ISE* as defined in (23) and (24), respectively, are calculated for all the input operating conditions at the end of the developed program and the results are analyzed. The values of these two performance indices help us to conclude the same inferences with regard to reactive power compensation of the studied hybrid power system model.

(d) *Analysis of time-domain responses*: Fig. 6 is pertaining to the comparative SIMULINK-based time-domain response profiles of ΔV_t (p.u.) for the studied test cases and the comparative algorithms with 1% step change in reference voltage for nominal input conditions like $V = 1.0$ p.u. and $X_{eq} = 0.93$ p.u.. Fig. 7 depicts the same for an another nominal input conditions like $V = 1.01$ p.u. and $X_{eq} = 1.08$ p.u. From these two figures, it is prominent that among the two test cases (viz. model and model + SVC), test Case II yields the optimal voltage response profile for the given nominal input operating condition and an adopted algorithm. This has happened with the help of true reactive power support from the SVC loop for test Case II which is absent for test Case I.

(e) *TSFL-based response:* For on-line, off-nominal input sets of parameters, TSFL model is utilized to get the on-line, optimal controller parameters and these controller parameters also yield the on-line incremental change in terminal voltage response profile (Fig. 8). Table 6 illustrates the Sugeno fuzzy-based off-nominal, on-line optimal parameters and values of *FOD*, *IAE*, *ISE*, and *ISTE* (using BGA-/HS-/OHS-based optimal parameters of Table 4) for on-line, off-nominal input sets of parameters. During real-time operation, the values of V and X_{eq} are determined from the system. For these sets of V and X_{eq} values, the optimal system parameters may be computed by using the fuzzy rule-based table and the Takagi–Sugeno inference system. Thus, the suitability of the proposed TSFL controller during real-time operation of the studied hybrid power system model is demonstrated.

(f) *Comparison of the optimizing algorithms*: Fig. 9 depicts time-domain responses of ΔV_t (p.u.) for the studied algorithms with 1% step perturbation in reference voltage for nominal input conditions as laid down. This figure, basically, portrays the comparative incremental change in terminal voltage as yielded by the different optimization techniques viz. BGA HS and OHS for test Case II. From this figure, it is clear that the OHS-based optimization yields true optimal reactive power compensation for the test Case II, i.e., model + SVC. Thus, the adopted hybrid power system model is truly compensated by the reactive power support for the proposed OHS-based approach.

(g) *Convergence profile*: Based on the same NFFEs, Fig. 10 portrays the comparative convergence profiles of the minimum P_{index} values yielded by the different comparative algorithms for a test Case II. From this figure, it

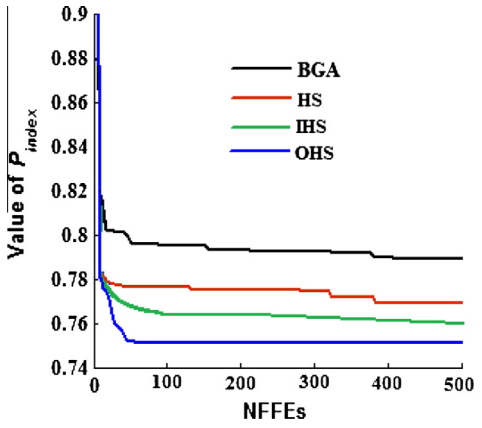

Figure 10 Comparative BGA-, HS-, IHS-, and OHS-based convergence profiles of minimum P_{index} values for Case II (Model + SVC) for nominal input condition of $V = 1.0$ p.u., $X_{eq} = 0.93$ p.u.

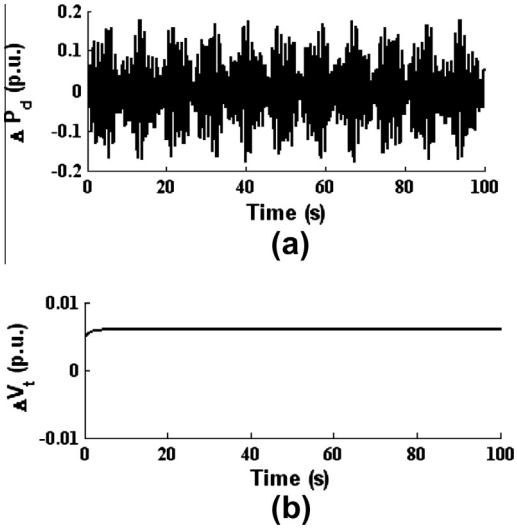

Figure 11 Dynamic performance evaluation: (a) applied sinusoidal load pattern and (b) OHS-TSFL-based time-domain simulation response of incremental change in terminal voltage (p.u.) for off-nominal input parameters like $V = 1.01$ p.u and $X_{eq} = 0.93$ p.u.

Table 7 Statistical analysis of results of different optimization techniques for the studied hybrid power system model for Case II viz. (Model + SVC) for an input operating condition of $V = 1.0$ p.u., $X_{eq} = 1.08$ p.u. over 30 independent trial runs.

Algorithms	Best	Worst	Mean	Std.	*t*-Value
BGA	0.7813	0.9979	0.8803	0.1463	6.2301
RGA	0.7800	0.9904	0.8901	0.1937	5.0633
HS	0.7735	0.7901	0.8250	0.1107	4.7013
IHS	0.7715	0.7802	0.7799	0.0599	3.3643
GHS	0.7608	0.7701	0.7692	0.0419	3.0039
SGHS	0.7506	0.7700	0.7649	0.0409	2.3339
OHS	**0.7472**	**0.7609**	0.7514	0.000186	**0**

Table A.1 Test functions.

Sl. no.	Name	Test function	n	Domain	Global optimum, x^*	Function value, $f(x^*)$
1	Sphere function	$f_1(x) = \sum_{i=1}^{n} x_i^2$	30	$[-100, 100]^n$	$[0]^n$	0
2	Schwefel's problem 2.22	$f_2(x) = \sum_{i=1}^{n} \lvert x_i \rvert + \prod_{i=1}^{n} \lvert x_i \rvert$	30	$[-10, 10]^n$	$[0]^n$	0
3	Rosenbrock function	$f_3(x) = \sum_{i=1}^{n-1} [100(x_{i+1} - x_i^2)^2 + (x_i - 1)^2]$	30	$[-30, 30]^n$	$[1]^n$	0
4	Step function	$f_4(x) = \sum_{i=1}^{n} (\lvert x_i + 0.5 \rvert)^2$	30	$[-100, 100]^n$	$[0]^n$	0
5	Rotated hyper-ellipsoid function	$f_5(x) = \sum_{i=1}^{n} \left(\sum_{j=1}^{i} x_j \right)^2$	30	$[-100, 100]^n$	$[0]^n$	0
6	Schwefel's problem 2.26	$f_6(x) = 418.9829 \times n - \sum_{i=1}^{n} x_i \sin\left(\sqrt{\lvert x_i \rvert} \right)$	30	$[-500, 500]^n$	$[420.96]^n$	0
7	Rastrigin's function	$f_7(x) = \sum_{i=1}^{n} [x_i^2 - 10\cos(2\pi x_i) + 10]$	30	$[-5.12, 5.12]^n$	$[0]^n$	0
8	Ackley's function	$f_8(x) = -20\exp\left(-0.2\sqrt{\frac{1}{n}\sum_{i=1}^{n} x_i^2} \right) - \exp\left(\frac{1}{n}\sum_{i=1}^{n} \cos(2\pi x_i) \right) + 20 + e$	30	$[-32, 32]^n$	$[0]^n$	0
9	Griewank function	$f_9(x) = \frac{1}{4000}\sum_{i=1}^{n} x_i^2 - \prod_{i=1}^{n} \cos\left(\frac{x_i}{\sqrt{i}} \right) + 1$	30	$[-600, 600]^n$	$[0]^n$	0
10	Six-hump Camel-back function	$f_{10}(x) = 4x_1^2 - 2.1x_1^4 + \frac{1}{3}x_1^6 + x_1x_2 - 4x_2^2 + 4x_2^4$	2	$[-5, 5]^n$	(0.08983, 0.7126)	−1.0316285
11	Shifted Sphere function	$f_{11}(x) = \sum_{i=1}^{n} z_i^2 + f_{bias\ 1}$, $z = x - o + 1$, $o = [o_1, o_2, \ldots\ldots, o_n]$: the shifted global optimum	30	$[-100, 100]^n$	o	-450, $f_{bias1} = -450$
12	Shifted Schwefel's problem 1.2	$f_{12}(x) = \sum_{i=1}^{n} \left(\sum_{j=1}^{i} z_j \right)^2 + f_{bias\ 2}$, $z = x - o + 1$, $o = [o_1, o_2, \ldots\ldots, o_n]$: the shifted global optimum	30	$[-100, 100]^n$	0	-450, $f_{bias2} = -450$
13	Shifted Rosenbrock function	$f_{13}(x) = \sum_{i=1}^{n-1} [100(z_i^2 - z_{i+1})^2 + (z_i - 1)^2] + f_{bias\ 3}$, $z = x - o + 1$, $o = [o_1, o_2, \ldots\ldots, o_n]$: the shifted global optimum	30	$[-100, 100]^n$	o	390, $f_{bias3} = 390$
14	Shifted Rastrigin function	$f_{14}(x) = \sum_{i=1}^{n} [z_i^2 - 10\cos(2\pi z_i) + 10] + f_{bias4}$, $z = x - o + 1$, $o = [o_1, o_2, \ldots\ldots, o_n]$: the shifted global optimum	30	$[-5, 5]^n$	o	-330, $f_{bias\ 4} = -330$
15	Shifted rotated Griewank's function	$f_{15}(x) = \frac{1}{4000}\sum_{i=1}^{n} z_i^2 - \prod_{i=1}^{n} \cos\left(\frac{z_i}{\sqrt{i}} \right) + 1 + f_{bias\ 5}$, $z = (x - o) \times M$, $o = [o_1, o_2, \ldots\ldots, o_n]$: the shifted global optimum, M is linear transformation matrix	30	$[-100, 100]^n$	o	-180, $f_{bias\ 5} = -180$
16	Shifted rotated Rastrigin function	$f_{16}(x) = \sum_{i=1}^{n} [z_i^2 - 10\cos(2\pi z_i) + 10] + f_{bias\ 6}$, $z = (x - o) \times M$, $o = [o_1, o_2, \ldots\ldots, o_n]$: the shifted global optimum, M is linear transformation matrix	30	$[-5, 5]^n$	o	-330, $f_{bias\ 6} = -330$

Please refer to the website http://www3.ntu.edu.sg/home/EPNSugan/ for the details of these test functions.

Table A.2 Data for the proposed hybrid power system model.

Synchronous generator	Induction generator	Load	SVC
$P_{sg} = 0.4$ p.u. kW	$P_{ig} = 0.6$ p.u. kW	$P_{load} = 1.0$ p.u. kW	$Q = 0.841$ p.u. kVAR
$Q_{sg} = 0.2$ p.u. kVAR	$Q_{ig} = 0.291$ p.u. kVAR	$Q_{load} = 0.75$ p.u. kVAR	$\alpha = 138.8^0$
$E_q = 1.12418$ p.u.	$P_{in} = 0.667$ p.u. kW	Power factor = 0.8	
$\delta = 17.2483^0$	$\eta = 90\%$		
$E'_q = 0.9804$ p.u.	Power factor = 0.9		
$V = 1.0$ p.u.	$r_1 = r'_2 = 0.19$ p.u.		
$X_d = 1.0$ p.u.	$x_1 = x'_2 = 0.56$ p.u.		
$X'_d = 0.15$ p.u.	$S = -3.5\%$		
$T'_{do} = 5.0$ s	–		

may be noted that the proposed OHS-based meta-heuristic offers faster convergence profile and also lesser final value of *ISTE* as compared to either BGA- or HS-based approach for this adopted test case. BGA yields suboptimal higher values of P_{index}.

(h) *Performance evaluation with sinusoidal load pattern*: The performance evaluation of the studied isolated hybrid power system model with sinusoidal load pattern and OHS-based optimization technique for on-line, off-nominal input sets of parameters is also carried out. The expression for the sinusoidal load change containing low sub-harmonic terms [24] is assumed as in (35) and its variation with time (for 100 s) is plotted in Fig. 11a.

$$\Delta P_d = 0.03\sin(4.36t) + 0.05\sin(5.3t) - 0.1\sin(6t) \quad (35)$$

Under the on-line, off-nominal input sets of parameters with sinusoidal load pattern, the TSFL extrapolates the nominal optimal parameters intelligently and linearly in order to determine the off-nominal optimal SVC controller parameters. These controller parameters yield the optimal incremental change in terminal voltage response profile as presented in Fig. 11b. From this figure, it may be noted that with the application of a continuously fluctuating load demand, smooth output voltage response profile is obtained with the assistance of a truly compensated reactive power support from the SVC loop.

(i) *Statistical analysis*: The *t*-values between the OHS and the other optimization methods are presented in Table 7. The *t*-value of all approaches is larger than 2.15 (degree of freedom = 49), meaning that there is a significant difference between the OHS and other methods with a 98% confidence level. BGA-based results yield suboptimal results. Thus, from statistical analysis, it is clear that the OHS-based optimization technique offers robust and promising results.

7. Conclusion

In this paper, the concept of opposition-based learning has been employed to accelerate the HS algorithm. The notion of opposition-based learning has been utilized to introduce opposition-based HM initialization and opposition-based generation jumping. By embedding these two steps within the HS, an opposition-based HS algorithm is proposed in this paper. The proposed algorithm is tested on sixteen benchmark test functions. The simulation results demonstrate the effectiveness and robustness of the proposed algorithm to solve the benchmark test functions. Moreover, the results of the proposed algorithm have been compared to those surfaced in the recent state-of-the-art literature. As an engineering optimization application, reactive power control of an isolated hybrid power system model is carried out with the help of the proposed OHS algorithm. From the simulation study, it is revealed that the proper tuning of the SVC yields the true optimal voltage response profile for the studied hybrid power system model. TSFL is applied to obtain the on-line output terminal voltage response. The comparison of the numerical results and the convergence profiles of the optimum objective function values confirm the effectiveness and the superiority of the proposed approach of the current article.

Appendix A

A.1. Description of benchmark test functions

Description of benchmark test functions is presented in Table A.1.

A.2. Power system data

The values of the different constants used for the simulation (Fig. 4) are $K_{a5} = 2V \times B_{svc}$, $K_v = 6.667$, $T = 7.855 \times 10^{-4}\,s$, $T_r = 0.02s$, $K_a = 200$, $T_a = 0.01$ s, $H = 1.0$, $D = 0.8$, $\omega_0 = 314$.

The other data of the studied hybrid isolated power system model are presented in Table A.2.

References

[1] Sarker R, Mohammadin M, Yao X. Evolutionary computations. New York: Kluwer Academic Publishers; 2003.
[2] Geem ZW, Kim JH, Loganathan GV. A new heuristic optimization algorithm: harmony search. Simulations 2001;76:60–8.
[3] Mahdavi M, Fesanghary M, Damangir E. An improved harmony search algorithm for solving optimization problems. Appl Math Comput 2007;188:1567–79.
[4] Lee KS, Geem ZW. A new structural optimization method based on the harmony search algorithm. Comput Struct 2004;82:781–98.

[5] Kim JH, Geem ZW, Kim ES. Parameter estimation of the nonlinear Muskingum model using harmony search. J Am Water Resource Assoc 2001;37:1131–8.
[6] Geem ZW, Kim JH, Loganathan GV. Harmony search optimization: application to pipe network design. Int J Model Simul 2002;22:125–33.
[7] Geem ZW, Lee KS, Park Y. Application of harmony search to vehicle routing. Am J Appl Sci 2005;2:1552–7.
[8] Geem ZW. Optimal cost design of water distribution networks using harmony search. Eng Optimiz 2006;38:259–80.
[9] Geem ZW. Optimal scheduling of multiple dam system using harmony search algorithm. New York: Springer-Verlag; 2007.
[10] Omran MGH, Mahdavi M. Global-best harmony search. Appl Math Comput 2008;198:643–56.
[11] Pan QK, Suganthan PN, Tasgetiren MF, Liang JJ. A self-adaptive global best harmony search algorithm for continuous optimization problems. Appl Math Comput 2010;216:830–48.
[12] Tizhoosh HR. Opposition-based learning: a new scheme for machine intelligence. In: Proc int conf comput intell modeling control and autom, vol. 1; 2005. p. 695–701.
[13] Tizhoosh HR. Reinforcement learning based on actions and opposite actions. In: Proc ICGST int conf artif intell mach learn. Egypt; 2005.
[14] Tizhoosh HR. Opposition-based reinforcement learning. J Adv Comput Intell Inform 2006;10:578–85.
[15] Ventresca M, Tizhoosh HR. Improving the convergence of back-propagation by opposite transfer functions. In: Proc IEEE world congr comput intell. Vancouver BC Canada; 2006. p. 9527–34.
[16] Rahnamayan S, Tizhoosh HR, Salama MMA. Opposition-based differential evolution. IEEE Trans Evol Comput 2008;12:64–79.
[17] Cheng JWM, Galiana FD, McGillis DT. Studies of bilateral contracts with respect to steady-state security in a deregulated environment. IEEE Trans Power Syst 1998;13(3):1020–5.
[18] Gajjar GR, Khaparde SA, Soman, SA. Modified model for negotiations in market games under deregulated environment. In: Proc 11th nat power syst conf. Bangalore, India; 2000. p. 222–8.
[19] Bansal RC, Bhatti TS, Kothari DP. Bibliographical survey on induction generators for application of non-conventional energy systems. IEEE Trans Energy Convers 2003;18(3):433–9.
[20] Hingorani NG, Gyugyi L. Understanding FACTs: concepts and technology of flexible AC transmission systems. New York: IEEE Power Eng. Soc.; 2000.
[21] Xi-Fan Wang, Song Y, Irving M. Modern power systems analysis. New York: Springer; 2008.
[22] Gaing ZL. A particle swarm optimization approach for optimum design of PID controller in AVR system. IEEE Trans Energy Convers 2004;19(2):384–91.
[23] Mukherjee V, Ghoshal SP. Intelligent particle swarm optimized fuzzy PID controller for AVR system. Electr Power Syst Res 2007;72(12):1689–98.
[24] Bhatt P, Roy R, Ghoshal SP. Comparative performance evaluation of SMES-SMES, TCPS-SMES and SSSC-SMES controllers in automatic generation control for a two-area hydro–hydro system. Electr Power Energy Syst 2011;33(10):1585–97.

Abhik Banerjee was born in 1986 at Burnpur, Burdwan, West Bengal, India. He received his B.Tech degree in electrical engineering from Asansol Engineering College (under West Bengal University of Technology), Asansol, Burdwan, India and M.Tech. in Power System from Dr. B.C. Roy Engineering College (under West Bengal University of Technology), Durgapur, Burdwan, India, respectively. Currently, he is working in the capacity of assistant professor in the department of electrical engineering, Asansol Engineering College, Asansol, West-Bengal, India. Now, he is pursuing his Ph.D. degree from Indian School of Mines, Dhanbad, Jharkhand, India. His research interest includes reactive power control, distributed generation, load tracking. He will be available at abhik_banerjee@rediffmail.com.

V. Mukherjee was born in 1970 at Raina, Burdwan, West Bengal, India. He received his graduation in electrical engineering and post graduation in power system from B.E. College, Shibpur, Howrah, India and B.E. College (Deemed University), Shibpur, Howrah, India, respectively. He received his Ph.D. degree from NIT, Durgapur, India. Presently, he is an assistant professor in the department of electrical engineering, Indian School of Mines, Dhanbad, Jharkhand, India. His research interest is application of soft computing intelligence to various fields of power systems He will be available at vivek_agamani@yahoo.com. Dr. Mukherjee is a member of The Institution of Engineers (India).

S.P. Ghoshal received B.Sc, B.Tech degrees in 1973 and 1977, respectively, from Calcutta University, India. He received M.Tech degree from IIT (Kharagpur) in 1979. He received Ph.D. degree from Jadavpur University in 1992. Presently, he is acting as Professor of Electrical Engineering Department of National Institute of Technology, Durgapur, West Bengal, India. His research interest is application of soft computing intelligence to various fields of power systems and antenna. He will be available at spghoshalnitdgp@gmail.com. Prof. Ghoshal is member of IEEE and fellow of The Institution of Engineers (India).